

PAPER

# Strong influence of the oxygen stoichiometry on the vortex bundle size and critical current densities $J_c$ of $\text{GdBa}_2\text{Cu}_3\text{O}_x$ -coated conductors grown by co-evaporation

To cite this article: N Haberkorn *et al* 2017 *Supercond. Sci. Technol.* **30** 095009

View the [article online](#) for updates and enhancements.

## Related content

- [Influence of random point defects introduced by proton irradiation on the flux creep rates and magnetic field dependence of the critical current density  \$J\_c\$  of co-evaporated  \$\text{GdBa}\_2\text{Cu}\_3\text{O}\_7\$  coated conductors](#)  
N Haberkorn, Jeehoon Kim, S Suárez *et al.*
- [Vortex creep and critical current densities  \$J\_c\$  in a 2  \$\mu\text{m}\$  thick  \$\text{SmBa}\_2\text{Cu}\_3\text{O}\_7\$ d coated conductor with mixed pinning centers grown by co-evaporation](#)  
N Haberkorn, Y Coulter, A M Condó *et al.*
- [Enhancement of the critical current density by increasing the collective pinning energy in heavy ion irradiated Co-doped  \$\text{BaFe}\_2\text{As}\_2\$  single crystals](#)  
N Haberkorn, Jeehoon Kim, K Gofryk *et al.*

## Recent citations

- [Strong-pinning regimes by spherical inclusions in anisotropic type-II superconductors](#)  
R Willa *et al*

# Strong influence of the oxygen stoichiometry on the vortex bundle size and critical current densities $J_c$ of $\text{GdBa}_2\text{Cu}_3\text{O}_x$ -coated conductors grown by co-evaporation

N Haberkorn<sup>1,2</sup>, J Guimpel<sup>1,2</sup>, S Suárez<sup>1,2</sup>, H Troiani<sup>1,2</sup>, P Granell<sup>3</sup>,  
F Golmar<sup>4</sup>, Jae-Hun Lee<sup>5</sup>, S H Moon<sup>5</sup> and Hunju Lee<sup>5</sup>

<sup>1</sup> Comisión Nacional de Energía Atómica and Consejo Nacional de Investigaciones Científicas y Técnicas, Centro Atómico Bariloche, Av. Bustillo 9500, 8400 San Carlos de Bariloche, Argentina

<sup>2</sup> Instituto Balseiro, Universidad Nacional de Cuyo y Comisión Nacional de Energía Atómica, Av. Bustillo 9500, 8400 San Carlos de Bariloche, Argentina

<sup>3</sup> INTI, CMNB, Av. Gral Paz 5445 (B1650KNA), San Martín, Buenos Aires, Argentina

<sup>4</sup> Consejo Nacional de Investigaciones Científicas y Técnicas, Escuela de Ciencia y Tecnología, UNSAM, Campus Miguelete, (1650), San Martín, Buenos Aires, Argentina

<sup>5</sup> SuNAM Co. Ltd, Ansung, Gyeonggi-Do 430-817, Republic of Korea

E-mail: [nhaberk@cab.cnea.gov.ar](mailto:nhaberk@cab.cnea.gov.ar)

Received 29 May 2017, revised 21 June 2017

Accepted for publication 3 July 2017

Published 11 August 2017



CrossMark

## Abstract

We report on the influence of oxygen stoichiometry on the vortex creep mechanism of  $\text{GdBa}_2\text{Cu}_3\text{O}_x$ -coated conductors produced by co-evaporation. The oxygen stoichiometry of the films,  $x$ , was modified in a controlled way between 6.85 and 7, which resulted in systematic and reversible control of the superconducting critical temperature between about 78 and 93 K. The change in the oxygen stoichiometry produces a strong reduction in the self-field critical current densities  $J_c$  without significantly modifying the power-law dependence at intermediate magnetic fields, which indicates a negligible contribution of oxygen vacancies to the pinning. In addition, the characteristic glassy exponent  $\mu$  shows a systematic diminution from about 1.63 at  $x = 7$  to about 1.12 at  $x = 6.85$ . The results are compared with those obtained for proton- and oxygen-irradiated films, in which the vortex dynamics is determined by a balance between the improved pinning, originating from nanocluster inclusion, and the suppressed superconducting properties due to disorder in the nanoscale.

Keywords: coated conductors, glassy exponents, vortex dynamics

(Some figures may appear in colour only in the online journal)

## 1. Introduction

A significant improvement of the in-field dependences of  $\text{RBa}_2\text{Cu}_3\text{O}_{7-\delta}$  (RBCO; R = Sm, Dy, Y, Gd) coated superconductors (CCs) can be obtained by proton or oxygen irradiation [1–3]. This irradiation introduces a high density of

nanoclusters, which assists vortex pinning by defects originating during the synthesis of the tapes (dislocation, boundaries between islands and nanoparticles). With adequate irradiation doses the critical current density  $J_c$  at high fields can be doubled compared with pristine tapes [1–3]. The optimal doses result from a balance between the enhancement

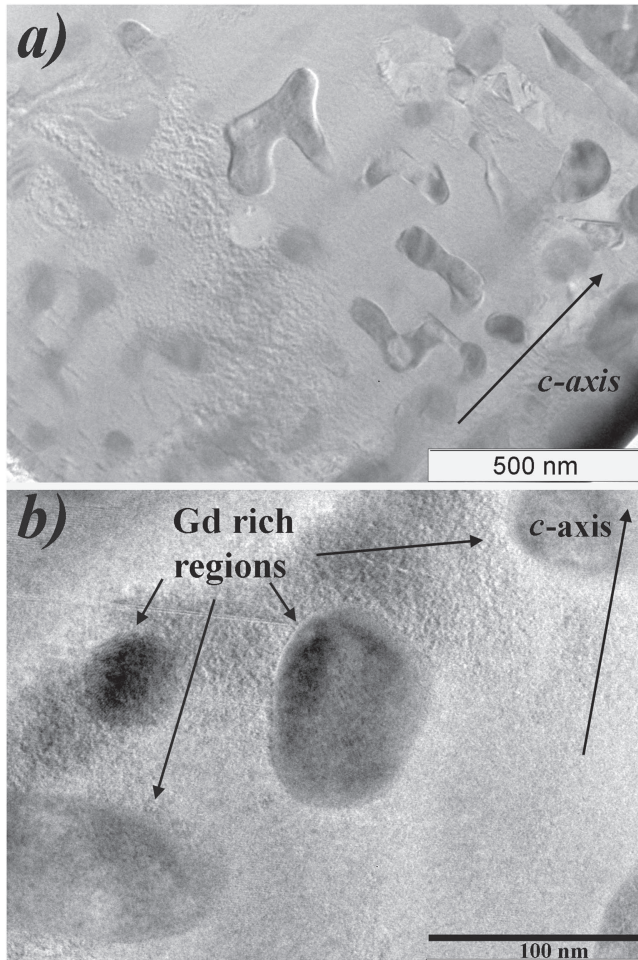


**Figure 1.** (a) A TEM image showing typical pinning centers in a GBCO tape. (b) A higher-magnification image showing spherical Gd-rich precipitates.

of the critical current densities  $J_c$  and the suppression of the superconducting properties produced by the damage. The disorder produced by the irradiation usually reduces the values of the superconducting critical temperature ( $T_c$ ) and the self-field  $J_c$  ( $J_{csf}$ ) [1–4]. Since structural disorder produced by irradiation should increase the penetration length ( $\lambda$ ) [5–7], depairing critical current density ( $J_0$ ), thermal fluctuations and the elasticity of the vortex lattice should be strongly affected [8]. The penetration depth  $\lambda$  in RBCO compounds can be modified by both irradiation-induced disorder [6] and changes in oxygen stoichiometry [9].

Another relevant feature for irradiated CCs is related to changes in the vortex dynamics when the doses are increased, which is manifested in the relaxation of the persistent critical currents [1–4, 10]. At intermediate and high temperatures, the inclusion of defects by irradiation usually suppresses the peak associated with double kinks (a fingerprint of correlated disorder) and produces an increment in the flux creep rates ( $S = -\partial \ln J / \partial t$ , with  $t$  being the time) [1, 2]. This suppression can be expected from random disorder avoiding the expansion of half-loops [11]. The increment in the flux creep rates seems counterintuitive, since more pinning would be expected to reduce its value [12]. Therefore, this increment at

intermediate temperatures requires further analysis. The plateau usually observed in cuprates at intermediate temperatures is related to glassy relaxation, characteristic of collective creep of vortex bundles [8]. For this mechanism, the normalized creep rate  $S$  is given by

$$S = \frac{T}{U_0 + \mu T \ln(t/t_0)} = \frac{T}{U_0} \left( \frac{J}{J_c} \right)^\mu \quad (1)$$

(equation (1)), where  $U_0$  is the characteristic energy,  $\mu > 0$  is the characteristic glassy exponent and  $t_0$  is a characteristic time. At intermediate temperatures,  $U_0 \ll \mu T \ln(t/t_0)$  and  $S$  is determined by the vortex bundle size as  $S \approx 1/[\mu \ln(t/t_0)]$ , with  $\ln(t/t_0) \approx 27$ –30. Pristine tapes usually have  $\mu \approx 1.6$ –1.7 [2, 4, 13, 14] and this value systematically drops with irradiation. For instance, the optimal dose of irradiation with 6 MeV oxygen reduces  $\mu$  to  $\approx 1.4$  [4]. The increment in the flux creep rates has been recently discussed considering the influence of the crystalline defects on the vortex bundle size [10]. For this study, the authors systematically removed crystalline defects by thermal annealing, which simultaneously modifies the vortex pinning and reduces the disorder produced by the irradiation (locally modifying the superfluid density [6]).

In this work, we modify the  $T_c$  of 1.3  $\mu\text{m}$  thick GdBCO tapes grown by co-evaporation by modifying the oxygen stoichiometry [15]. The microstructure of pristine films displays, embedded in the GBCO matrix, sphere-like and irregular precipitates with typical diameter of approximately 50 nm spaced between 100 and 200 nm [4]. By changing the oxygen stoichiometry, modifications in  $T_c$  and  $\lambda$  without major changes in the pinning landscape are expected to occur [9]. The magnetic field dependence of  $J_c$  and the vortex dynamics of films with  $T_c$  between 78 and 93 K were analyzed by performing magnetization measurements. It was noted that the flux creep rates of the films strongly change with the reduction of  $T_c$ . Although a higher contribution of random point disorder to the vortex pinning is expected from oxygen vacancies, no appreciable contribution was observed. The results show that  $J_{csf}$  values are strongly suppressed as  $T_c$  decreases. In addition, the characteristic glassy exponent  $\mu$  systematically decreases with  $T_c$ . These features are similar to those observed in irradiated CCs, strongly suggesting that the performance of CCs is significantly affected by reduction of  $T_c$ .

## 2. Material and methods

The GBCO tape was grown by the co-evaporation technique as previously described [16]. The oxygen content  $x$  of the tapes was adjusted to the desired value by using the iso-stoichiometric annealing method [15]. The sample was heated in  $\text{O}_2$  at a pressure of 11.5 Torr at an annealing temperature  $T_{\text{ann}}(x)$  determined by the desired stoichiometry (445  $^\circ\text{C}$  for  $x = 6.85$  and 410  $^\circ\text{C}$  for  $x = 6.96$ ). After 2 h the film was slowly cooled down at a rate of 1  $^\circ\text{C min}^{-1}$ , while the  $\text{O}_2$  pressure was continually adjusted to follow the corresponding constant- $x$  line in the  $\text{O}_2$  pressure versus  $T$  phase diagram.

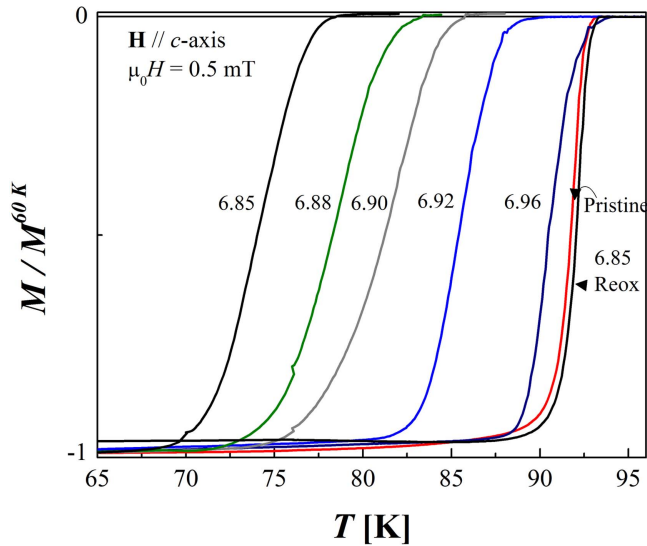


**Figure 2.** Temperature dependence of magnetization at  $\mu_0 H = 0.5$  mT in pristine and oxygen-deficient GBCO films. The magnetization value was normalized by its value at 60 K. The magnetic field was applied parallel to the  $c$ -axis.

The magnetization ( $M$ ) measurements were performed using a superconducting quantum interference device (SQUID) magnetometer with the applied magnetic field ( $H$ ) parallel to the  $c$ -axis ( $\mathbf{H}||c$ ). The  $T_c$  values used in this work, obtained from magnetization data, were determined from  $M(T)$  at  $\mu_0 H = 0.5$  mT after zero-field cooling. The  $J_c$  values were calculated from the magnetization data using the appropriate geometrical factor in the Bean model. For  $\mathbf{H}||c$ ,  $J_c = 20\Delta M/[w(1 - w/3l)]$ , where  $\Delta M$  is the difference in magnetization between the top and bottom branches of the hysteresis loop and  $l$  and  $w$  are the length and width of the film ( $l > w$ ), respectively. The  $M$  versus time curves were recorded for more than 1 h. The initial time was adjusted considering the best correlation factor in the log–log fitting of the  $J_c(t)$  dependence. To ensure a critical state, the initial state for each measurement was generated using a field variation  $\Delta H \sim 4H^*$ , where  $H^*$  is the field for full-flux penetration [17]. The microstructure of the films was analyzed by transmission electron microscopy (TEM) using a CM200 UT microscope operated at 200 kV. For TEM analysis, a thin lamella was prepared with a gallium-focused ion beam (FEI Helios Nanolab 650).

### 3. Results and discussion

The microstructure of the GBCO tapes was previously studied, and the results are discussed in [4]. Figure 1(a) shows a cross-sectional TEM image where sphere-like and irregular precipitates embedded in the GBCO matrix are identified. Figure 1(b) shows a higher-magnification image with several sphere-like precipitates. Energy dispersive spectroscopy analysis indicates that these regions are rich in Gd, which can be associated with  $Gd_2O_3$ . Figure 2 shows the temperature dependence of the normalized magnetization for films with  $x = 6.85, 6.88,$

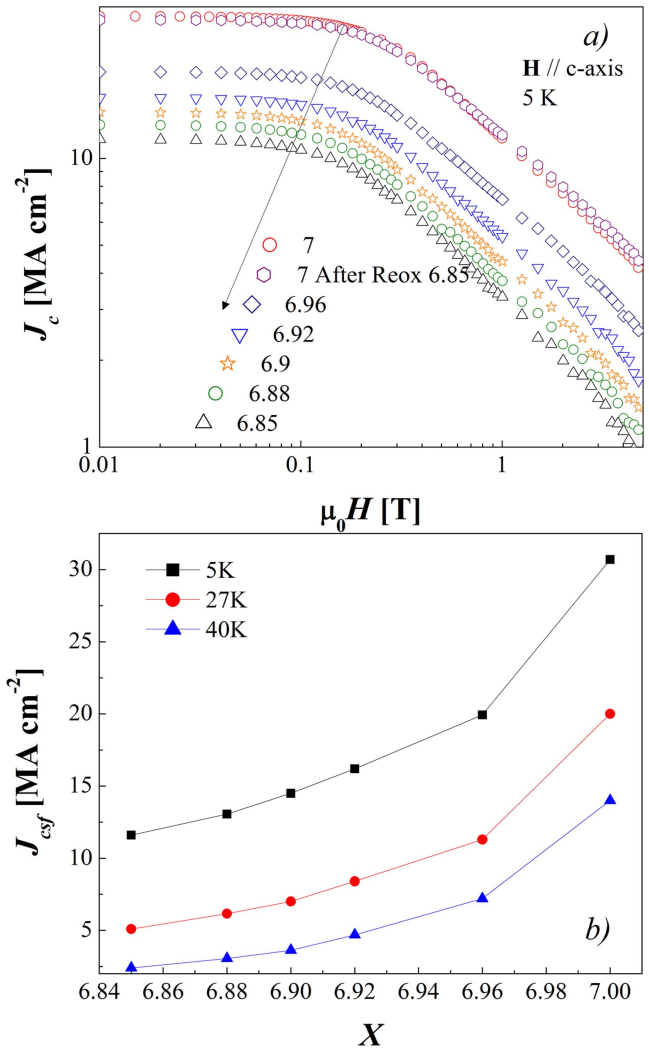


**Figure 3.** (a) Magnetic field dependence of the critical current density for films with different oxygen content  $x$  at 5 K. All measurements were performed with  $\mathbf{H}||c$ . (b) Self-field critical current density  $J_{csf}$  as function of  $x$  at 5, 27 and 40 K. Error bars in  $J_c$  are  $\approx 7\%$ .

6.9, 6.92, 6.96 and 7. The  $T_c$  values systematically decrease from  $\approx 93$  K (pristine) to  $\approx 78$  K. In addition,  $T_c \approx 93$  K is recovered after reoxygenation. Figure 3(a) shows a comparison between  $J_c(H)$  at 5 K for films with different  $x$ . The curves display two different regimes. At low fields  $J_c$  is almost independent of field up to a characteristic crossover  $H^*$ , usually called  $B^*$  [18]. Then, it is followed by a power-law regime ( $J_c \propto H^{-\alpha}$ ) at intermediate fields, observed as a linear dependence on the log–log plot. The main change produced by  $T_c$  is related to the drop in  $J_{csf}$ . On the other hand, a negligible influence of  $x$  is observed in the power-law regime. In irradiated samples [1, 2],  $\alpha$  drops with the different doses. Unlike these samples, the value of  $\alpha$  remains almost constant ( $\approx 0.64$ ) at 5 K, which indicates a negligible contribution to the vortex pinning of random point defects produced by oxygen vacancies. This insubstantial contribution indicates that the main changes produced in the in-field dependence of proton- and oxygen-irradiated CCs are mainly produced by nanoclusters [1–3]. On the other hand, similar  $J_c(H)$  dependences in a pristine film and a

reoxygenated  $x = 6.85$  are observed at different temperatures (see figure 3(a)), which indicates that no significant changes in the pinning landscape are produced by thermal annealing. Figure 3(b) shows the  $x$  dependence (related to  $T_c$ ) of the  $J_{csf}$  values at  $T = 5, 27$  and  $40$  K. A similar behavior is observed for the analyzed temperatures:  $J_{csf}$  drops systematically with reduction in the oxygen content. The suppression of  $J_{csf}$  is remarkable even for small changes in oxygen content. For instance, at  $5$  K and  $x = 6.96$ , there is a decrease close to 40% in comparison with pristine film and the  $T_c$  value drops to almost 1 K. This indicates that the modification in  $T_c$  has a significant affect on the vortex pinning and the intrinsic superconducting properties of the films. Although different types of disorder can be expected from the modification of the oxygen content (vacancies) and by irradiation (vacancies and random nanoclusters), the disorder in the nanoscale has a noticeable effect on the superfluid density,  $\rho_s = (\lambda(0)/\lambda(T))^2$  [6], and on the related superconducting parameters [8], such as the depairing critical current ( $J_0 = cH_c/3\sqrt{6\pi}\lambda$ , with  $H_c$  the thermodynamic critical field and  $c$  the speed of light) and the Ginzburg number,  $Gi = \frac{1}{2}(\gamma T_c/H_c^2(0)\xi^3(0))^2$ , with  $\xi_{ab}$  the coherence length and  $\gamma$  the mass anisotropy). The value of  $Gi$  determines the strength of the thermal fluctuations and is directly related to thermal depinning of vortices. For optimally doped samples  $Gi \approx 0.01$  ( $T_c = 93$  K and  $\lambda(0) \approx 120$  nm) and increases when  $T_c$  drops, and  $\lambda$  and  $\gamma$  increase. In addition, the flux creep mechanism is also affected by the ratio  $J_c/J_0$ , which is a parameter that characterizes the strength of the disorder potential [8]. An increment in  $\lambda(0)$  from 120 nm to 150 nm is expected in YBCO single crystals when  $T_c$  drops from  $\approx 92$  K to  $\approx 82$  K by modifying  $x$  [9], which implies that  $J_0$  should be reduced by around 35%. For oxygen-deficient samples it is expected that both the reduction of  $J_0$  and the increment in the vortex fluctuation ( $Gi$ ) contribute to the drop in the  $J_c$  value. For proton- and oxygen-irradiated CCs [1–3], the inclusion of nanoclusters improves the vortex pinning, which is evidenced in larger  $J_c$  values at high magnetic fields. This enhancement in the pinning is expected to compensate the large suppression of  $J_{csf}$  observed in oxygen-deficient samples. It is worth mentioning that while, for fully oxygenated YBCO, the anisotropy parameter  $\gamma$  takes values between 5 and 7, it is known to increase when the oxygen content is reduced [19, 20]. The gradual change in  $\gamma$  with  $x$  is expected to affect the vortex pinning (changing  $Gi$ ), which for highly oxygen-deficient samples ( $T_c < 50$  K and  $x < 6.48$ ) is evidenced in a vortex crossover from three-dimensional (3D) to a pure two-dimensional (2D) vortex-glass [21].

In order to analyze and compare the vortex dynamics in oxygen-deficient and oxygen-irradiated films [2, 4], magnetic relaxation measurements were performed at  $\mu_0 H = 0.5$  T. Figure 4(a) shows the  $S(T)$  dependences for films with different oxygen doping. The initial increment of  $S(T)$  at low temperatures can be ascribed to an Anderson–Kim-like mechanism with  $S \approx T/U$  ( $U$  being the pinning energy). Non-negligible  $S$  values are expected at  $T = 0$  from quantum creep [8]. When  $x$  is reduced, the initial slope at low temperatures is increased, which suggests a drop in  $U$ . On the other hand, the temperature for the peak ( $\approx 20$  K) is usually

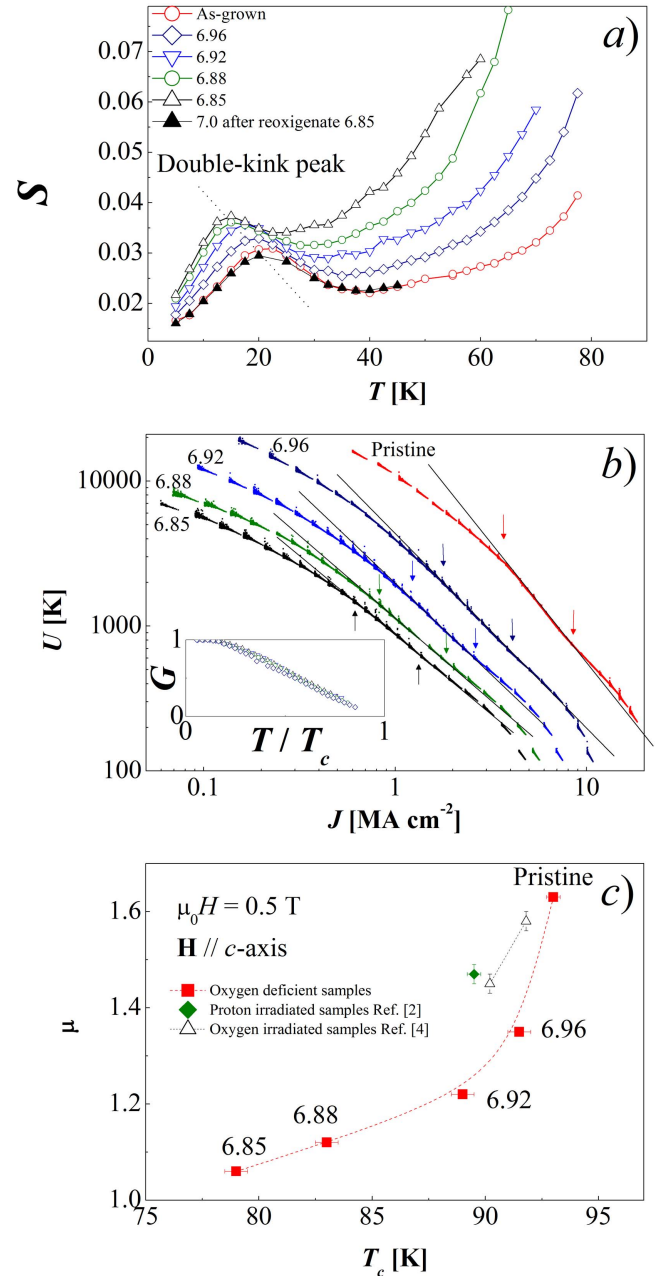


**Figure 4.** (a) Temperature dependence of the creep flux rate ( $S$ ) at  $\mu_0 H = 0.5$  T for films with different oxygen stoichiometry. The dotted line corresponds to the maximum temperature for the double-kink peak. (b) Maley analysis at  $\mu_0 H = 0.5$  T for films with different oxygen doping. The arrows indicate the range of  $J$  where the characteristic glassy exponent  $\mu$  was obtained. (c) Oxygen doping dependence of  $\mu$  values obtained from (b).

associated with double kinks and it systematically shifts when  $x$  is reduced (see dotted line in figure 4(a)). Considering the weak temperature dependence of the parameters  $\xi$ ,  $\lambda$  and  $\gamma$ , the peak by double-kink excitation is expected to occur at the same  $J_c/J_0$  ratio [22]. For example, the temperature for the peak in the pristine film is  $\approx 22$  K and  $J_c \approx 8$   $\text{MA cm}^{-2}$ , whereas for  $x = 6.85$  the peak for  $\mu_0 H = 0.5$  T occurs at  $\approx 15$  K and  $J_c \approx 2.2$   $\text{MA cm}^{-2}$ . In YBCO single crystals, for  $x = 6.95$ ,  $\lambda(20 \text{ K}) \approx 130$  nm ( $T_c \approx 92$  K) and for  $x = 6.8$ ,  $\lambda$

(20 K)  $\approx 155$  nm ( $T_c \approx 82$  K) [9], which suggests that the reduction in  $J_c$  at the peak is consistent with a reduction in  $J_0$  produced by an increment in  $\lambda$  due to the change in  $x$ . At temperatures higher than the peak associated with double kinks, the  $S(T)$  dependences plateau. When  $x$  decreases, a systematic increment in the absolute  $S$  value is observed, which can be related to a drop in the  $\mu$  value. Finally, at even higher temperatures,  $S$  increases rapidly as the system crosses over into the plastic regime [23]. For the oxygen-deficient films it is expected that this crossover will be affected by the changes in  $\lambda$  and  $\gamma$  [23]. It is worth mentioning that reoxygenated films display  $S(T)$  behavior similar to that of pristine films, which indicates that no significant modifications in the pinning landscape are introduced during the thermal annealing and that the main changes can be associated with modifications in the superfluid density of the films [9].

The glassy exponent  $\mu$  was analyzed using the extended Maley's method [24] so as to compare the modifications in the vortex dynamics for GBCO CCs introduced by oxygen doping modification and those observed in tapes irradiated with protons and oxygen ions. Considering the approximation in which the current density decays as  $\frac{dJ}{dr} = -\left(\frac{J_c}{\tau}\right) \exp(-U_{\text{eff}}(J)/T)$ , the effective activation energy  $U_{\text{eff}}(J)$  can be experimentally obtained by

$$U_{\text{eff}} = -T \left[ \ln \left| \frac{dJ}{dr} \right| - C \right] \quad (2)$$

(equation (2)), where  $C = \ln(J_c/\tau)$  is nominally a constant factor. For an overall analysis it is necessary to consider the function  $G(T)$ , which results in

$$U_{\text{eff}}(J, T = 0) \approx U_{\text{eff}}(J, T)/G(T) \quad (3)$$

(equation (3)) [25]. Figure 4(b) shows the results obtained for  $x = 6.85, 6.88, 6.92, 6.96$  and a pristine film. The inset shows  $G(T/T_c)$ . In the limit of  $J \ll J_c$  the  $\mu$  exponent can be estimated as  $\Delta \ln U(J)/\Delta \ln J$  [22]. The  $\mu$  values obtained at intermediate temperatures as function of  $T_c$  and  $x$  are summarized in figure 4(c). In addition, the characteristic glassy exponent  $\mu$  for tapes irradiated with protons and oxygen ions were included [2, 4]. The results indicate that  $\mu$  is systematically reduced with  $x$  from  $\mu \approx 1.63$  for the pristine tape to  $\mu \approx 1.12$  for  $x = 6.85$ . The model of vortex loop nucleation for the 3D case and for random point defects predicts  $\mu = 1/7$  for single-vortex creep,  $\mu = 3/2$  or  $5/2$  for small-bundle creep, and  $\mu = 7/9$  for large-bundle creep [8]. Although different characteristic glassy exponents  $\mu$  can be expected for mixed pinning landscapes, pristine films display  $\mu$  values close to those predicted for small bundles. The change in the oxygen content reduces the  $\mu$  values, in agreement with irradiated samples. The differences in the absolute value of  $\mu$  between oxygen-deficient and irradiated samples may originate in the differences in the pinning landscapes. It is worth noting that unlike for films irradiated with proton and oxygen ions, with remarkable changes in the in-field  $J_c$  dependences, no appreciable contribution of oxygen vacancies to the pinning has been observed ( $\alpha$  is weakly affected).

Studies in clean YBCO single crystals with low  $J_c$  values have shown that unlike CCs, the reduction in  $T_c$  with  $x$  weakly affects the glassy exponent  $\mu \approx 0.9$  [22]. This fact

indicates that the influence of the disorder on the vortex dynamics is different in strong-pinning (mixed pinning landscapes) and weak-pinning samples. This can be associated with the fact that changes in the glassy exponent  $\mu$  are related to both  $\lambda$  (related to  $T_c$ ) [6, 9] and  $J_c$  (related to the type of pinning center [10]). To our knowledge, there are no theoretical predictions of vortex bundle size and crossover between vortex regimes for samples with mixed pinning landscapes. Since high  $J_c$  values can be expected from an adequate combination of pinning centers, controlled modification of the size of dispersed defects and their influence on superconducting properties (such as superfluid density) should contribute to optimize pinning in CCs. Systematic determination of  $\lambda$  values and correlation vortex dynamics of pristine and irradiated films are necessary.

## 4. Conclusions

In summary, the influence of oxygen stoichiometry on the resulting vortex dynamics of 1.3  $\mu\text{m}$  thick  $\text{GdBa}_2\text{Cu}_3\text{O}_{7-\delta}$ -coated conductors was studied. Our results show that small changes in  $T_c$  have a significant effect on vortex pinning, which is manifested in a strong reduction of the  $J_{\text{csf}}$  values. In addition, the flux creep rates at intermediate and high temperatures show a systematic increment when  $x$  is reduced. This fact can be associated with a reduction in the characteristic glassy exponent  $\mu$ . A reduction in both  $J_{\text{csf}}$  and  $\mu$  values is usually observed in proton- and oxygen-irradiated CCs. This fact indicates a non-negligible contribution of the disorder produced by the irradiation in the final performance of irradiated tapes.

## Acknowledgments

This work was partially supported by Agencia Nacional de Promoción Científica y Tecnológica PICT 2015-2171. NH and JG are members of the Instituto de Nanociencia y Nanotecnología—CNEA (Argentina).

## References

- [1] Jia Y *et al* 2013 *Appl. Phys. Lett.* **103** 122601
- [2] Haberkorn N, Kim J, Suárez S, Lee J-H and Moon S H 2015 *Supercond. Sci. Technol.* **28** 125007
- [3] LeRoux M *et al* 2015 *Appl. Phys. Lett.* **107** 192601
- [4] Haberkorn N *et al* arXiv:1706.04228
- [5] Basov N *et al* 1994 *Phys. Rev. B* **49** 12165
- [6] Franz M, Kallin C, Berlinsky A J and Salkola M I 1997 *Phys. Rev. B* **56** 7882
- [7] Uemura Y J *et al* 1989 *Phys. Rev. Lett.* **62** 2317
- [8] Blatter G, Feigelman V B, Geshkenbein V B, Larkin A I and Vinokur V M 1994 *Rev. Mod. Phys.* **66** 1125
- [9] Sonier J E *et al* 2007 *Phys. Rev. B* **76** 134518
- [10] Eley S, Leroux M, Rupich M W, Miller D J, Sheng H, Niraula P M, Kayani A, Welp U, Kwok W-K and Civale L 2017 *Supercond. Sci. Technol.* **30** 015010
- [11] Civale L 1997 *Supercond. Sci. Technol.* **10** A11
- [12] Haberkorn N *et al* 2012 *Phys. Rev. B* **85** 174504

- [13] Haberkorn N *et al* 2016 *Supercond. Sci. Technol.* **29** 075011
- [14] Polat O *et al* 2011 *Phys. Rev. B* **84** 025519
- [15] Osquiguil E, Maenhoudt M, Wuyts B and Bruynseraede Y 1992 *Appl. Phys. Lett.* **60** 1627
- [16] MacManus-Driscoll J L *et al* 2014 *APL Mater* **2** 086103
- [17] Yeshurun Y, Malozemoff A P and Shaulov A 1996 *Rev. Mod. Phys.* **68** 911
- [18] van der Beek C J *et al* 2002 *Phys. Rev. B* **66** 024526
- [19] Chien T R *et al* 2004 *Physica C* **229** 273
- [20] Takenaka K, Mizuhashi K, Takagi H and Uchida S 1994 *Phys. Rev. B* **50** 6534
- [21] Sefrioui Z Z *et al* 1999 *Phys. Rev. B* **60** 15423
- [22] Thompson J R, Krusin-Elbaum L, Civale L, Blatter G and Field C 1997 *Phys. Rev. Lett.* **78** 3181
- [23] Abulafia Y *et al* 1996 *Phys. Rev. Lett.* **77** 1596
- [24] Maley M P, Willis J O, Lessure H and McHenry M E 1990 *Phys. Rev. B* **42** 2639
- [25] Ossandon J G *et al* *Phys. Rev. B* **46** 3050